Synthesis and study the structure, optical, thermal and dielectric properties of promising Glycine Copper Nitrate (GCN) single crystals

Ollaa M. Mailoud[a,*], Adly H. Elsayed[b], A.H. Abo-Elazm[b], H.A. Fetouh[c]

[a] Department of Physics, Faculty of Science, Benghazi University, Libya
[b] Department of Physics, Faculty of Science, Alexandria University, Egypt
[c] Department of Chemistry, Faculty of Science, Alexandria University, Egypt

ABSTRACT

Four novel single crystals of α-glycine and γ-glycine doped by copper nitrate: $(Glycine)_{1-x} (Cu(NO_3)_2 \cdot 3H_2O)_x$ abbreviated as (GCN1, GCN2, GCN3, GCN4) were prepared from aqueous solution by the slow evaporation method. Four doping concentrations: x = 0.005, 0.01, 0.02 and 0.04 of hydrated copper nitrate were used. The crystals were studied using powder X-ray diffraction (PXRD), Fourier Transform Infrared Spectroscopy (FTIR), and UV–Vis spectroscopy. The PXRD patterns showed that crystals containing high concentration of $Cu(NO_3)_2 \cdot 3H_2O$ have triclinic or monoclinic structure. The lattice parameters for all the prepared crystals were found to be in a good agreement with that found in the crystallographic open database (COD). The functional groups of the crystals were determined from FTIR spectra and the optical band gaps were calculated from UV–Vis spectroscopy technique. The properties of the crystals was found to be concentration dependent on copper nitrate salt. The refractive index (n) for all GCN crystals were found around 1.88 in the region of the wavelength: 800–1000 nm, while the least value of $n \approx 1.72$ was determined in the visible region of electromagnetic magnetic radiation. The decomposition point of GCN single crystals was identified by a narrow, and sharp peak of differential scanning calorimetry (DSC) curves. The phase transition temperature at 203 °C was observed for GCN2 crystals, is probably due to the transformation from γ-glycine to α-glycine. The dielectric study showed a peak around 30 °C (Curie temperature) that is a characteristic of ferroelectric crystals and the consistency of the dielectric constant at 90 °C indicated glass transition. Photoluminescence spectra of GCN crystals that were recorded at the excitation wavelength of 280 nm showed a maximum emission peaks around 345 nm. This finding indicated that these single crystals can be successfully used for NLO applications.

Introduction

The organometallic or semiorganic single crystals of glycine have wide non-linear optical (NLO) applications and exhibit ferroelectricity, piezoelectricity and pyroelectricity. These crystals were extensively used in optoelectronics such as optical amplifiers, laser crystals, light modulation and optical memory storage [1–3]. Single crystals were classified into three types: organic, inorganic and semiorganic materials. Semioganic crystals can be prepared from amino acid as organic ligands combined with transition metal ions. Some metals complex of amino acids exhibit ferroelectric properties due to the polarity these amino acid. Glycine is the simplest amino acid, it was used successfully in the growth of single crystals. It can be appeared in α, β and γ glycine polymorphs at the ambient conditions [4,5]. The more stable γ-glycine crystals were grown from aqueous solutions in the presence of additives

of transition metal salts [6–8].Many authors were reported the growth of γ-glycine as semiorganic materials with chloride salts [9–12], While the growth of α-glycine as semiorganic materials was obtained by the spontaneous nucleation from pure aqueous glycine solution [13–16]. The α-glycine was reported as the least stable crystals than other polymorphs of glycine in aerated conditions. The (NLO) properties for glycine copper chloride and glycine copper sulphate single crystals were investigated and the optical band gaps (E_g) were calculated [17,18].

This work aims to grow novel GCN single crystals and by slow evaporation method and characterize these crystals using elemental analysis, FTIR spectra, UV–Vis spectroscopy, powder XRD, dielectric study, thermal analysis (DSC) and Photoluminescence analysis (PL).

* Corresponding author at: Physics Department, College of Arts and Sciences, Benghazi University, Libya.
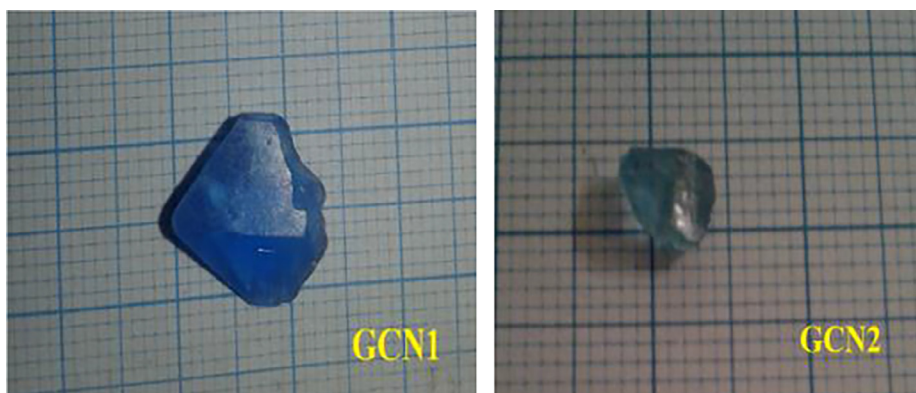E-mail address: barga_2012@yahoo.com (O.M. Mailoud).

Fig. 1a. γ-Glycine of GCN with x = 0.005, 0.01.

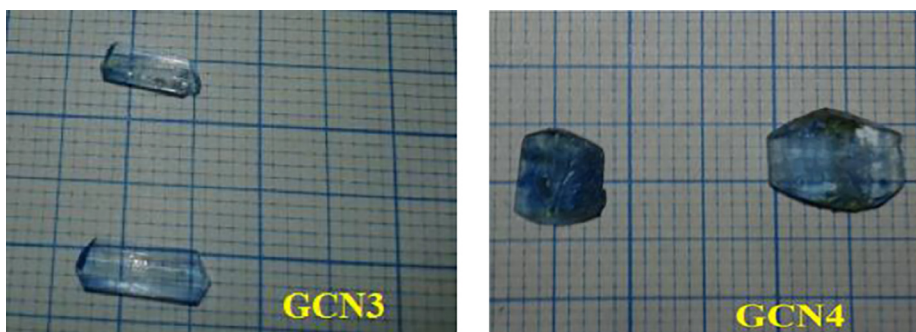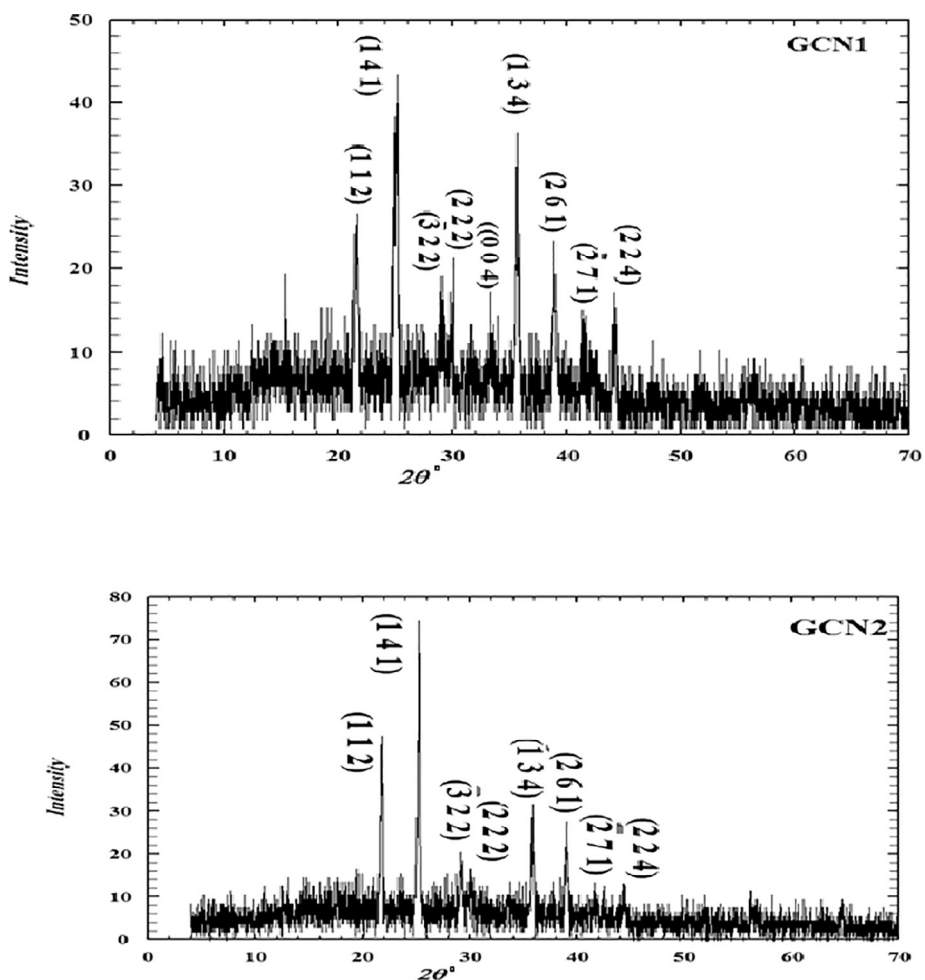**Fig. 1b.** α-Glycine of GCN with x = 0.02, 0.04.

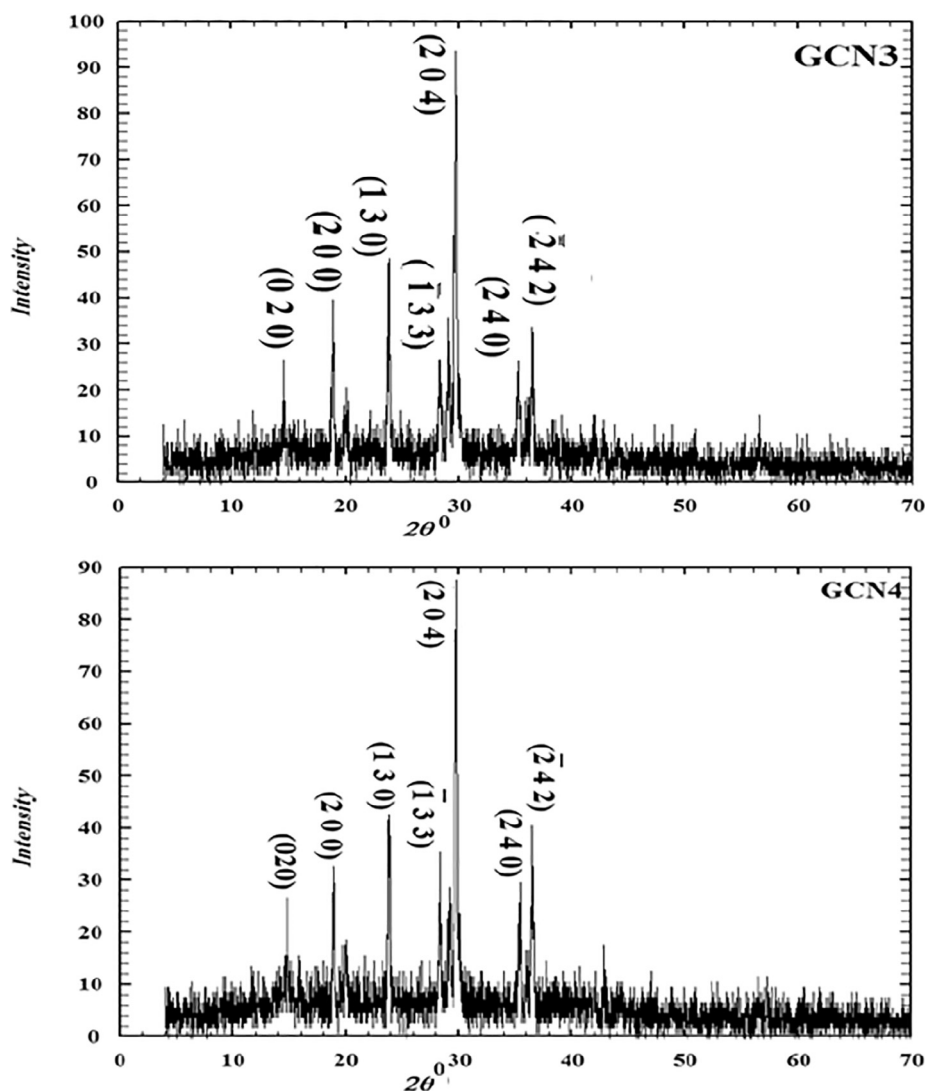**Fig. 2a.** Indexed powder XRD profile of (α)-GCN.

Fig. 2b. Indexed powder XRD profile of (α)-GCN.

Experimental

Single crystals of Glycine Copper Nitrate (GCN) were grown using glycine ($C_2H_5NO_2$) (Oxford) of purity (98.5%), and $Cu(NO_3)_2 \cdot 3H_2O$ of purity (98%) (Aldrich). Four single crystals $(Glycine)_{1-X} (M)_X$, where M represents $Cu(NO_3)_2$ with the molar percent: x = 0.005, 0.01, 0.02 and 0.04 which denotes (GCN1, GCN2, GCN3, GCN4) respectively. The appropriate weights of all powder solids were dissolved in double distilled water to get a saturated solution, then the solution was stirred for two hours after heated to about 45 °C. The solution was filtered and covered with a porous paper. A digital pH meter (AD11 type) was employed for recording pH of the solution. Then the solution was kept in a dust free environment, the pH and the temperature of the solution were in the range of 3.7–5 and 40–45 °C respectively. Good quality single crystals of GCN were appeared with a blue color which harvested after 30 days. The solvent had been evaporated and GCN crystals with different dimensions were obtained. Fig. 1 showed the relative dimensions of both γ -glycine, and α-glycine single crystals. It was found that the higher molar concentrations of copper enhanced the nucleation than the lower molar concentrations in a good agreement with the results for other single crystals [19]. The structure of the grown crystals was confirmed by the PXRD using a Bruker (AXS) instrument with CuK_α radiation (1.5406 Å), the sample was scanned at 25 °C in the angle range: 5° to 70° by step 0.02° on applying scan rate of 1° min^{-1}. FTIR spectrum was recorded by (SHIMADZU) instrument in the range 450–4000 cm^{-1}. The UV–Visible spectrum was studied using UV-Spectrophotometer (Helios, Unicam) spectrophotometer.

The ferroelectric behavior of GCN single crystals was confirmed by the dielectric study as a function of temperature in the range (25–180 °C) and at the frequency ranges from: [100 Hz to 100 kHz] using LRC bridge of type Tesla 6472. The DSC analysis was studied using SHIMADZU (DSC 60) under nitrogen atmosphere, the rate of heating was 20 °C/min at the temperature range: 25–400 °C. Photolumeneces (PL) spectrometer of the type (Perkin-Elmer model IS 55) was used in recording the emission spectra from the crystal. Elemental analysis (EA) of these samples were done to determine the ratios of CHN and hence deduce the empirical formula of the crystals.

Results and discussions

Powder XRD results

The PXRD pattern for glycine doped copper nitrate single crystals is shown in Fig. 2(a, b). A sharp and strong peak appeared in each concentration as one dominating peak confirming the good quality of the grown semiorganic crystals. The indexed PXRD parameters are shown in Table 1. Structure type and the lattice parameters of the crystals are shown in Table 2. From this Table Triclinic or Monoclinic structures

Table 1
The indexed powder X-ray diffraction pattern for GCN at different concentrations.

	$2\theta_{(EXP)}$	$d(A)_{(EXP)}$	$(h k \ell)$	Intensity %
GCN1	21.564	4.11763	(1 1 2)	58.5
	25.13	3.54084	(1 4 1)	100
	28.997	3.07685	($\bar{3}$ 2 2)	32.6
	29.876	2.98832	(2 2 2)	26.9
	33.255	2.69195	(0 0 4)	28.6
	35.644	2.51683	(1 3 4)	70.1
	38.898	2.31342	(2 6 1)	43.1
	41.366	2.180093	($\bar{2}$ 7 1)	21.2
	44.271	2.04434	(2 2 4)	29.5
GCN2	21.753	4.08227	(1 1 2)	67.2
	25.233	3.52663	(1 4 1)	100
	29.179	3.05808	($\bar{3}$ 2 2)	28.8
	30.078	2.96864	(2 2 2)	19.5
	35.833	2.50397	(1 3 4)	43.8
	39.009	2.30709	(2 6 1)	34.7
	44.355	2.04064	(2 2 4)	20.4
GCN3	14.685	6.02739	(0 2 0)	19.3
	18.875	4.69777	(2 0 0)	38.4
	23.816	3.73317	(1 3 0)	46.8
	28.33	3.14773	($\bar{1}$ 3 3)	29.5
	29.123	3.06382	(0 4 0)	32.8
	29.722	3.00338	(2 0 4)	100
	35.271	2.54259	(2 4 0)	27.5
	36.493	2.46019	($\bar{2}$ 4 2)	32.5
GCN4	14.803	6.11835	(0 2 0)	18.7
	19.97	4.54828	(2 0 0)	18.9
	23.85	3.72186	(1 3 0)	49.2
	28.335	3.15947	($\bar{1}$ 3 3)	32.9
	29.139	3.5918	(0 4 0)	30.6
	29.768	2.99038	(2 0 4)	100
	35.332	2.53841	(2 4 0)	28.2
	36.493	2.46268	($\bar{2}$ 4 2)	40.5

Table 2
Powder XRD parameters for Glycine Copper Nitrate (GCN) single crystals.

The molar ratio of Glycine and Copper nitrate	GCN1 x = 0.005	GCN2 x = 0.01	GCN3 x = 0.02	GCN4 x = 0.04
Identifier	4,500,255		4,501,392	
Crystal system	Triclinic		Monoclinic	
Polymorph	Gamma(γ)		Alpha(α)	
Space group	P2₁		C2/c	
Lattice parameter	a = 10.439 Å		a = 9.1256 Å	
	b = 16.863 Å		b = 12.2367 Å	
	c = 11.302 Å		c = 17.072 Å	
	α = 90°		α = 90°	
	β = 107.84°		β = 94.572°	
	α = 90°		α = 90°	
Volume (A³)	1893.86		1900.32	

obtained at high dopant concentration. The software of Full Prof Suite (FPS) was used to calculate Miller indices (h k ℓ) as shown in Table 1. At concentrations (x = 0.005, 0.01) both crystals are Triclinic with space group P2₁, while at x = 0.02, and 0.04 both are Monoclinic structure of space group (C₂/c). The preferred orientation are (1 4 1) and (2 0 4) planes as observed for γ and α glycine respectively.

Elemental analysis (EA)

The ratio of Carbon, Hydrogen and Nitrogen (CHN) in the prepared crystal GCN1 as a representative example were determined using (CHN) analysis, the recorded values are presented in Table 3 and the empirical formula of this crystal was suggested to be: ($C_3H_9N_2O$).

FTIR spectral analysis

The characteristic vibrations bands of the carboxylate ions and the zwitter ionic group NH_3^+ of pure glycine and GCN1, GCN2, GCN3, GCN4 single crystals respectively are shown in Fig. 3(a, b). FTIR spectra of glycine showed the absorption band of (O–H) of carboxyate group and amino group in the frequency region (3500–4000) cm^{-1}. All the spectra of GCN crystals showed an absorption band of (O–H) of carboxyate group and amino group in the frequency region (3500–4000) cm^{-1} and a strong peak denoted to presence the copper nitrate, NH_3^+ bonding and another functional groups such as COO^-, NH_2, NH^{3+} CCN are also shown. The bending and rocking vibrations bands appeared as very strong peaks of COO^- group. The details of these are recorded in Table 4.

UV–Vis spectra

The UV spectroscopy of GCN crystals are shown in Fig. 4. The optical absorption spectra were recorded in the wavelength region (190–1200 nm) using sample solution. Fig. 4 showed that the samples have a high optical transmission in the visible region which are essential properties of the amino acids [20]. The inset represents the position of λ_{cut}(nm) as given in Table 5. The NLO activity of the crystals were confirmed through the determination of the cut-off wavelength that were found to lower than that of pure glycine [21], as shown in Table 5. The wide energy band gap of the grown crystal was shown in Fig. 5.

Since the optical constants play an important role in designing of optoelectronic devices. Hence it is necessary to determine these constants for GCN. The optical absorption coefficient (α) was calculated using the relation [11]:

$$\alpha = \frac{2.3042A}{t} \tag{1}$$

where: A is the absorbance, and t is the thickness of the sample.

The optical band gap can be estimated using the mathematical relation [22]:

$$\alpha h\upsilon = A(h\upsilon - Eg)^r \tag{2}$$

where: υ the frequency of the incident radiation, A is a constant and r is an index depending on the nature of the electronic transition responsible for the absorption. Where r = 2 signifies the indirect transition, and r = ½ signifies the direct transition. On taking, r = ½ (for allowed direct transition) and the optical gap, E_g was evaluated by plotting $(\alpha h\upsilon)^2$ as a function of photon energy (hυ) as shown Fig. 5 observed E_g are given in Table 5. The reflectance R parameter was calculated using the equation [23]:

$$R = 1 \pm \frac{\sqrt{1 - \exp(-\alpha t) + \exp(\alpha t)}}{1 + \exp(-\alpha t)} \tag{3}$$

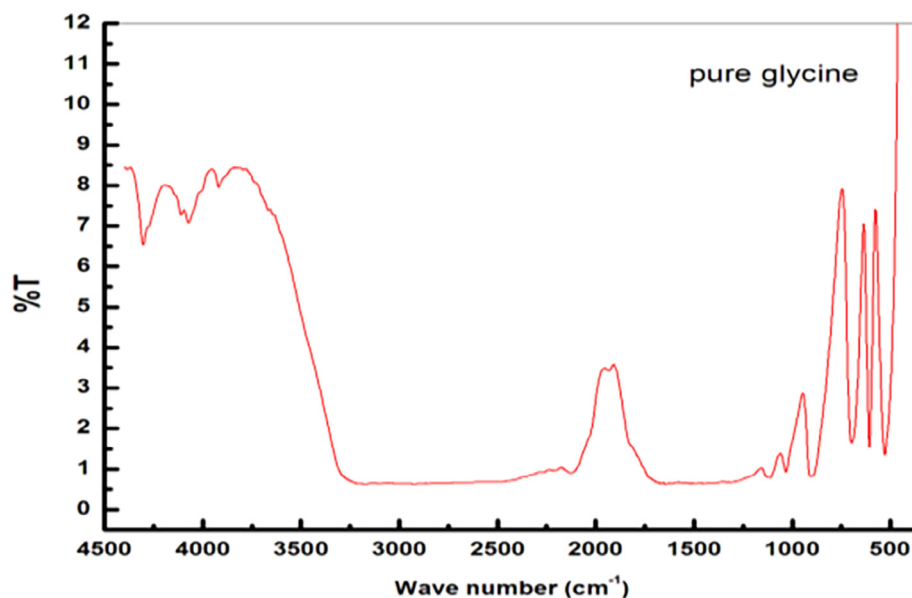The refractive index (n) of the crystal is related to reflectance R

Table 3
Elemental analysis of C, H, N in the single crystal GCN1.

C%	H%	N%	O%	n_{carbon}	$n_{hydrogen}$	$n_{nitrogen}$	n_{metal} X 10⁵	n_{oxygen}	C_{ratio}	H_{ratio}	N_{ratio}	O_{ratio}
39.36	9.2	34.50	17.0	3.28	9.08	2.46	23.6*	1.06	3.1	8.6	2.3	1.0

* Given from atomic absorption measurement.

Fig. 3a. FTIR spectrum of pure glycine single crystals.
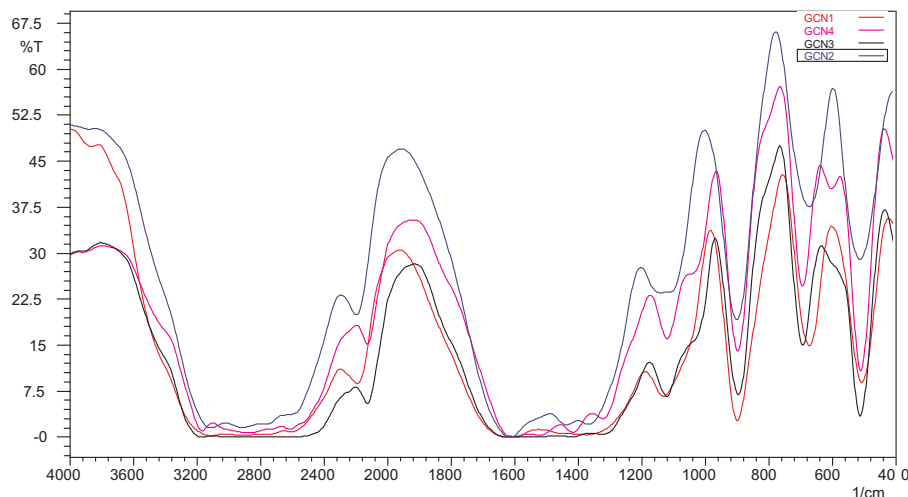

Fig. 3b. FTIR spectrum of GCN single crystals at different concentrations of Cu (NO$_3$)$_2$.

Table 4
Functional groups of Glycine Copper Nitrate single crystals.

Mode frequency	Wave number (cm^{-1})				
	Pure glycine	GCN1	GCN2	GCN3	GCN4
Bending and rocking vibrations of CO group	527.66	499.83	511.15	511.15	509.22
CO bending vibration	606.3–696.9	606.54	671.25	692.47	601.81
C−N symmetric stretching	–	892.51	898.86	895	896.93
C−N asymmetric stretching	1031.93–1112.44	1030.79–1109.98	1139.97	1120.68	1120.68
Symmetric stretching of CO	1311.89–1492.39	1329.89–1410.24	1367.58	1323.21	1321.28–1415.80
			1437.02	1408.08	
Asymmetric stretching of carbonyl group CO and NH$^+$ deformation	1554.25	1515.03	1599.04	1521.89	1519.96
NH$^+$ stretching	2126.40	2123.21	2195.07	2125.63	2125.63
C−H stretching	2924.04	2967.03	2912.61	2883.68	2883.68
Cu−N stretching	–	3167	3113.21	3171.08	3167.22
NH stretching	3921.39	3921.75	3878.98	3919.48	3921.41

which can be calculated from the equation [24,25]:

$$n = -\frac{(R + 1) \pm \sqrt{3R^2 + 10R - 3}}{2(R-1)} \qquad (4)$$

The recorded wide optical band gap of GCN crystals (Fig. 6) indicated that these crystals can be used in optoelectronic applications [8]. Fig. 6 represents the refractive index (n) versus wavelength for GCN single crystals. It is noticed that the crystals have a positive
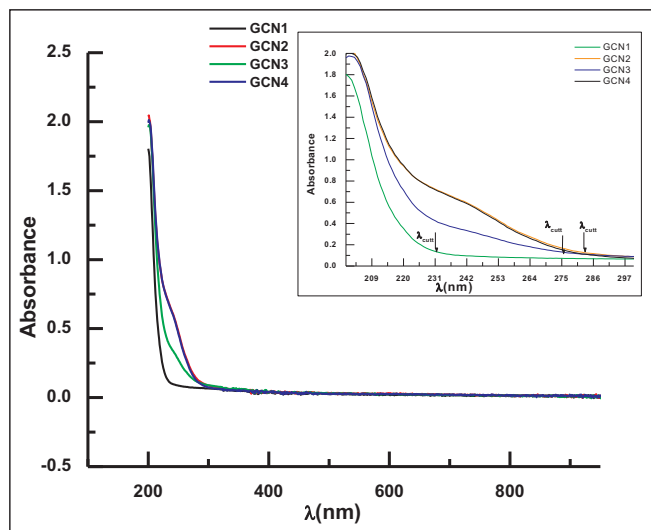
Fig. 4. The absorption spectra of GCN at different concentrations of $Cu(NO_3)_2$.

Table 5
Energy band gap E_g and λ_{cut} (nm) of GCN single crystals.

	GCN1	GCN2	GCN3	GCN4
E_g (eV)	5.77	5.62	5.69	5.64
λ_{cut} (nm)	231	282	275	282

refractive index, which is inversely proportional to photon energy and directly proportional to the wavelength. The refractive index for GCN crystals equals 1.88 over a wide range of wavelength (800–1000) nm, while less refractive index found in visible region (n = 1.72). This finding suggesting these materials are suitable for fabrication of solar thermal devices and NLO applications.
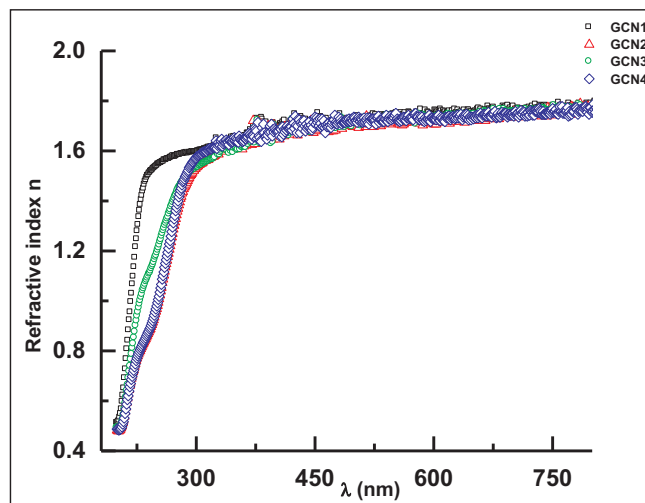

Fig. 6. The dependence of refractive index with wavelength for GCN single crystals.

Diffrentional scanning caliometery (DSC) results

The recorded DSC thermograms for GCN1 crystals were shown in Fig. 7 to illustrate: the thermal stability of this sample the heat flow (milli Watt) with the temperature in Celsius and the type (ΔH) exothermic or endothermic as well as thermal transition (glass temperature, T_g and Curie temperature, T_c). Narrow endothermic peaks for all concentrations were observed indicating the thermal decomposition of the samples [24]. The broad peak around 203 °C in sample GCN2, is characteristics for the phase change from γ-glycine to α-glycine before the material melts [25–28], The melting points of GCN crystals are shown in Table 6.
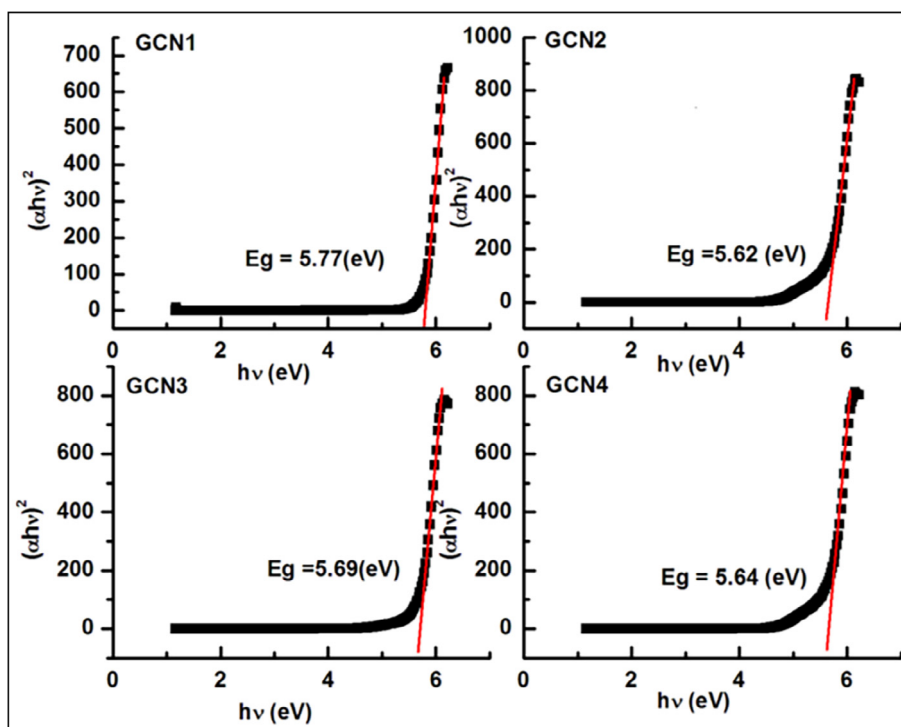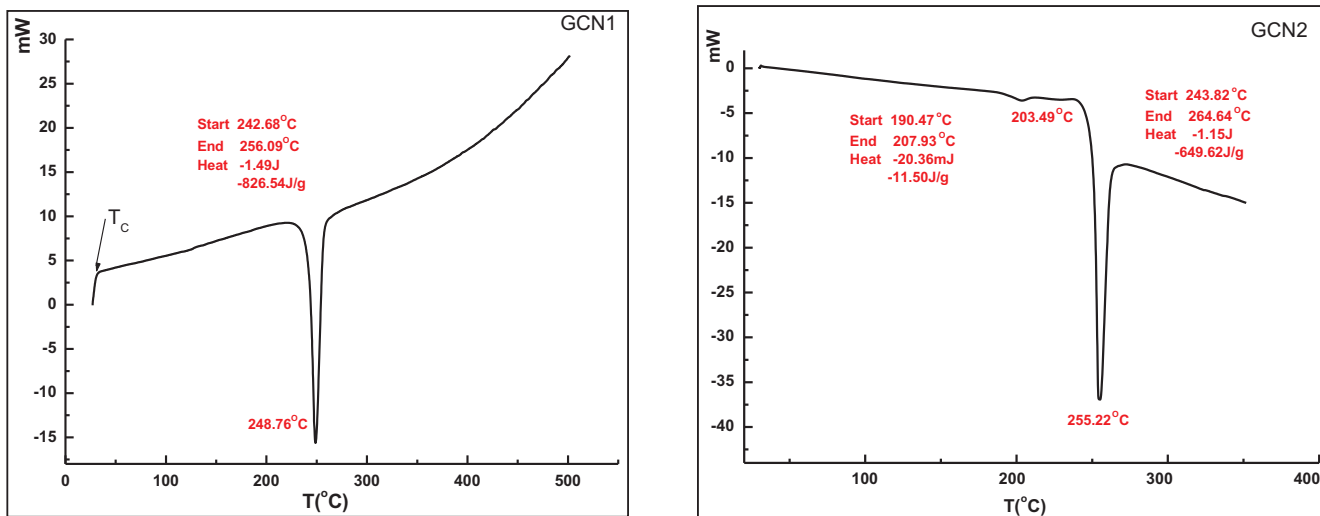

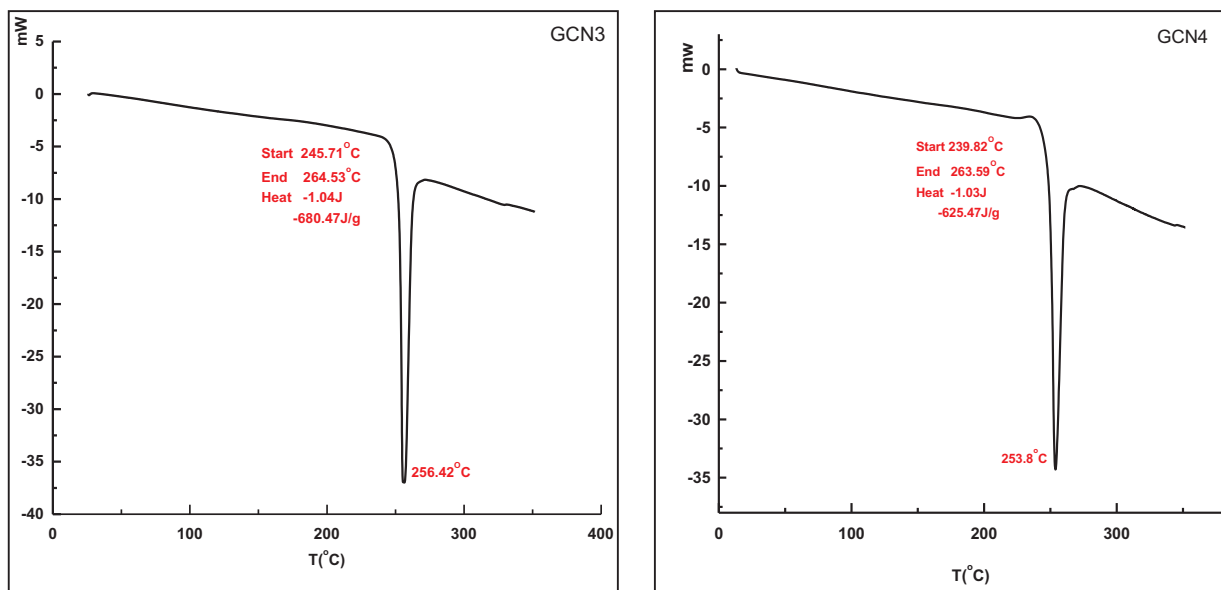**Fig. 5.** Tauc's plot of GCN crystals.

Fig. 7a. DSC curves of (γ)-glycine.

Fig. 7b. DSC curves of (α)-glycine.

Table 6
The decomposition temperature of GCN crystals as recorded from DSC measurements.

Sample	GCN1	GCN2	GCN3	GCN4
Decomposition temperature	248.76 °C	255.22 °C	256.42 °C	253.8 °C

Dielectric study

The objective of the dielectric study of GCN crystals have been carried to describe the response of charges in the GCN crystals to the external electric applied field. This study is the important analysis to understand the nature of the atoms and their bonding in the crystalline material [29], it is one of the basic electrical properties of solids. Good quality single GCN1 crystal was selected for the dielectric measurements at 100 Hz, 1 kHz,10 kHz, 100 kHz at the temperature range 19–180 °C. The sample form as a pellet with radius (0.5 cm), the thickness and the area of the samples were about 0.23×10^{-2} m and 7.854×10^{-5} m^2 respectively. The pellet was coated in two opposite surfaces by silver paste to attain good Ohmic contact with copper electrodes. The sample was annealed by putting them between two copper electrodes inside furnace at 120 °C (before starting the experiment).

The dielectric constant was calculated using the following equation [30–32]

$$\varepsilon = \frac{Cd}{\varepsilon_o A} \tag{5}$$

where ε_o is the free space permittivity, the real ε' and the imaginary ε'' parts of the dielectric constant are calculated according to:

$$\varepsilon' = |\varepsilon|\cos\Theta$$
$$\varepsilon'' = |\varepsilon|\sin\Theta \tag{6}$$

where C and d are the capacitance and the thickness of the pellet, A is the electrode area. Fig. 8 shows the variation of dielectric constant (ε') with temperature at different frequency, It is noticed that the dielectric values decreases with increasing frequency, this behavior gives an improved optical quality with fewer defects related to as anomalous dielectric dispersion sample. The values of ε' decreased until reached to the glass transition T_g at about 363 K, and then temperature
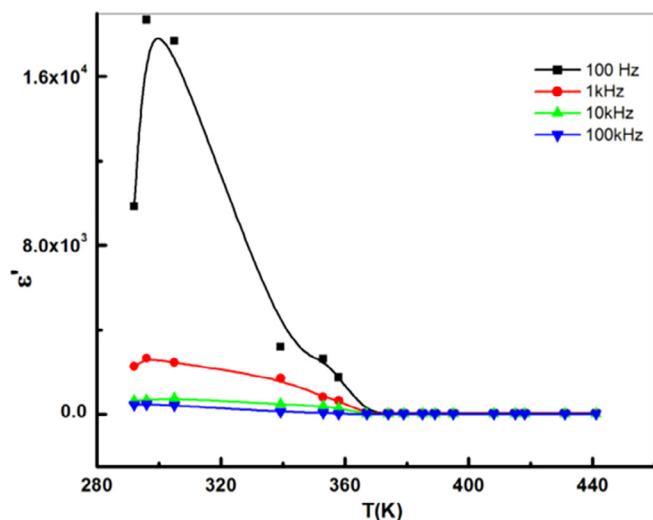
Fig. 8. Temperature dependent of the dielectric constant for (GCN1) single crystal. Solid line is guide to the eye.
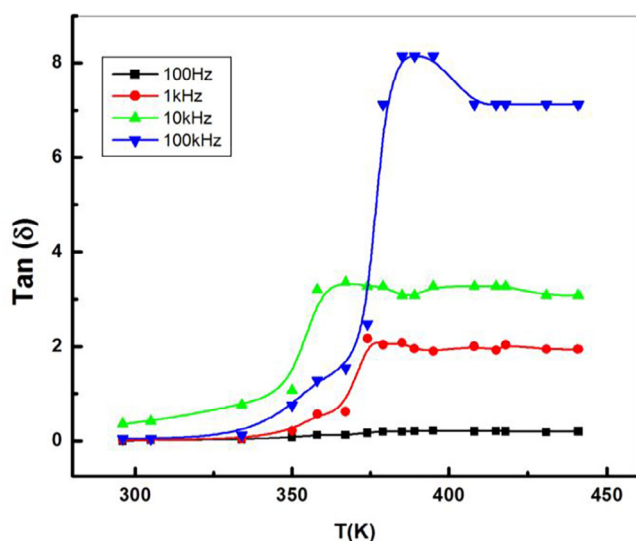

Fig. 9. The temperature dependence of dielectric loss of GCN1 single crystal at different frequency. Solid line is guide to the eye.
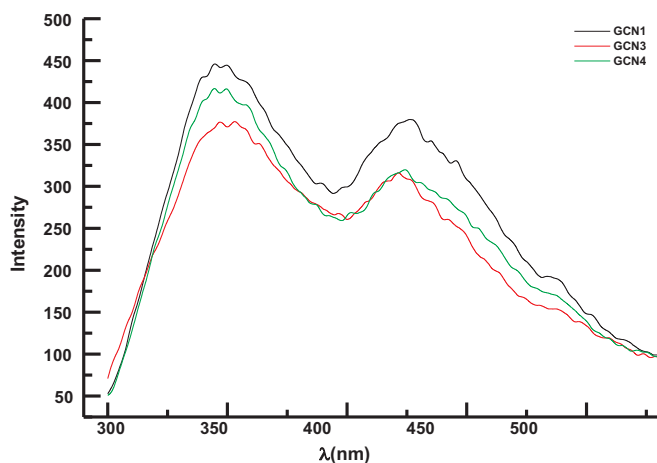

Fig. 10. Photoluminescence spectrum of GCN1, GCN3, GCN4 (excitation wavelength = 280 nm).

independent of ε′ was observed up to 440 K. It is noticed that the a peak near the room temperature at T = 30 °C represented the transition from ferroelectric to paraelectric behavior, T_C.

There is no shift in the ferroelectric Curie point shown in Fig. 8, they have almost the same peak position at different frequencies. The high value of the recorded dielectric constant may due to the presence of transition metal ions Cu^{2+} in the crystalline structure [33], or the presence of an oxygen vacancies. Fig. 9 shows the variation of dielectric loss (tan δ) with the temperature. The variation of dielectric loss as a function of real and imaginary parts of dielectric constant can be described by the equation:

$$tan\delta = \frac{\varepsilon''}{\varepsilon'} \qquad (7)$$

In general, the high value of dielectric constant and low dielectric loss at high frequency, confirmed that the sample possesses good optical quality which enhanced by the presence of fewer crystalline defects [34]. It is noticed that the dielectric constant decrease continuously with increasing the frequency, but dielectric losses rising strongly as a function of the frequency, the reason may be due to the switching response of the dipoles which cannot follow the oscillation of electric field at higher frequency [35].

Photoluminescence analysis (PL)

The study of the grown crystal by the photoluminescence analysis considers as a probe to the electronic structure of materials [36]. The photoluminescence spectrum of three GCN crystals were recorded in the wavelength range 300–600 nm at the room temperature at the excitation wavelength of 280 nm. Fig. 10 showed two emission broad peaks at about 345 and 425 nm. The peak at 345 nm was observed in the emission spectrum which corresponding to 3.6 eV of energy. The maximum intensity peak at 345 nm is due to the protonation of amino group from the proton of the carboxyl group. The lowering of photoluminescence intensity at higher wavelength region (425 nm) may be attributed to low barrier rotation C−C bond axis extend from central C to the carbon atom of the carboxyl group [37].

The details of the structure determination GCN crystals have been summarized as follows

The infrared spectra of glycine and GCN crystals are assigned to the position of the fundamental functional groups. These spectral studies confirmed that glycine ligand act as bidentate ligand with copper ion through one or two carbonyl oxygen, nitrogen atom glycine and nitrate group. The vibrational modes of the functional groups are described.

The geometries of GCN crystals were suggested from Powdered (XRD) of confirmed the definite crystalline nature of GCN crystals.

Conclusion

Single crystals of GCN have been successfully grown by the slow evaporation method in four different concentrations of $Cu(NO_3)_2 \cdot 3H_2O$. The PXRD showed a structural change from Triclinic (γ-glycine) to Monoclinic (α-glycine) as the concentration of copper nitrate increased. The observed cut-off wavelength of GCN crystals less than pure glycine which means that the crystals have higher transparency than pure glycine crystal. The optical band gap was calculated and is found to be in the range of 5.77–5.62 eV depending on the concentration of copper nitrate. The calculated refractive index is about 1.88 in high wavelength region (800–1000) nm while it is equal to 1.72 in visible region. The dielectric constant and dielectric loss was varied with the temperature and the frequency where the ferroelectric phase transition may be observed near 30 °C and a glass transition at 90 °C. Photoluminices measurements showed a strong emission peak at about 3.6 eV far from the obtained optical band gap. DSC measurement indicates the decomposition temperature of GCN crystals at about 250 °C in the latter measurement.

Appendix A. Supplementary data

Supplementary data associated with this article can be found, in the online version, at https://doi.org/10.1016/j.rinp.2018.05.042.

References

[1] Juliet Sheela K, Radha Krishnan S, Shanmugam VM, Subramanian P. Effect of VO^{2+} ions on the EPR and optical absorption investigations of lithium sulphate monohydrate single crystals for non linear optical applications. J Mol Struct 2017;1143:245–50.

[2] Anne MM, Perumal S, Prabu KM. Growth, structtural and optical studies on pure and L-HISTIDINE doped single crystals of Copper sulphate. Int J Res Eng Technol 2015;4(7):2319–7308.

[3] Damodaran P, Mahadevan M, Anandan P, Shanmugha Sundaram P, Rajasekaran R. Growth, structural, thermal and dielectric studies of alfa-glycine single crystals grown under the influence of potassium iodide for nonlinear optical applications. Adv Mater Proc 2017;2(2):80–5.

[4] Mahalingam T, Ravi G. Structural, functional and optical studies on the amino acid doped glycine crystal. AIP Conf Proc 2012;1447:1273. https://doi.org/10.1063/1.4710476.

[5] Renuka Devi K, Srinivasan K. Towards a better understanding of the nucleation behavior of alpha and gamma polymorphs of glycine from aqueous solution in the presence of selective additives by charge compensation mechanism. J Cryst Growth 2014;401:227–32.

[6] El-fadl AA, Abdulwahab AM. The effect of cobalt-doping on some of the optical properties of glycine zinc sulfate (GZS) single crystal. Phys B Phys Condens Matter 2010;405(16):3421–6.

[7] Selvarajan P, Glorium Arul Raj J, Perumal S. Characterization of pure and urea-doped γ-glycine single crystals grown by solution method. J Cryst Growth 2009;311(15):3835–40.

[8] Ashok Kumar R, Ezhil Vizhi R, Sivakumar N, Vijayan N, Rajan Babu D. Crystal growth, optical and thermal studies of nonlinear optical γ-glycine single crystal grown from lithium nitrate. Opt – Int J Light Electron Opt 2012;123(5):409–13.

[9] Palaniswamy S, Balasundaram ON. Effect of ph on the growth and characterization of Glycine Sodium chloride (GSC) single Crystal. Rasayan J 2009;2(0974-1496):386–92.

[10] John J, Christuraj P, Anitha K, Balasubramanian T. Band gap enhancement on metal chelation: Growth and characterization of cobalt chelated glycine single crystals for optoelectronic applications. Mater Chem Phys 2009;118(2–3):284–7.

[11] Dillip GR, Bhagavannarayana G, Raghavaiah P, Deva Prasad Raju B. Effect of magnesium chloride on growth, crystalline perfection, structural, optical, thermal and NLO behavior of gamma-glycine crystals. Mater Chem Phys 2012;134(1):371–6.

[12] Boopathi K, Rajesh P, Ramasamy P. Growth of negative solubility lithium sulfate monohydrate crystal by slow evaporation and Sankaranarayanan-Ramasamy method. J Cryst Growth 2012;345(1):1–6.

[13] Sugandhi K, Verma S, Jose M, Joseph V, Das SJ. Effect of pH on the growth, crystalline perfection, nonlinear optical and mechanical properties of tris-glycine zinc chloride single crystals. Opt Laser Technol 2013;54:347–52.

[14] Uma J, Rajendran V. Growth and characterization of gamma-glycine single crystals from cadmium chloride for optoelectronic applications. Optik (Stuttg) 2014;125(2):816–9.

[15] Balakrishnan T, Babu RR, Ramamurthi K. Growth, structural, optical and thermal properties of gamma glycine crystal. Spectrochim Acta Part A 2008;69:1114–8.

[16] Renuka Devi K, Gnanakamatchi V, Srinivasan K. Attainment of unstable Beta nucleation of glycine through novel swift cooling crystallization process. J Cryst Growth 2014;400:34–42.

[17] Sudha S, Sathya T, Raj MBJ. Studies on thermal, microhardness and di-electric properties of glycine nickel chloride. Int J Sci Technol Res 2012;1(10):35–7.

[18] Nalini Jayanthi DSS, Prabhakaran AR, Thamizharasan K. Crystallization and characterization of NLO active. Chalcogenide Lett 2014;11(5):241–7.

[19] Azhagan SAC, Ganesan S. Effect of zinc acetate addition on crystal growth, structural, optical, thermal properties of glycine single crystals. Arab J Chem 2013.

[20] Sugandhi K, Selvambikai M, Shobhana E. Optik growth, non-linear optical, photoconductivity and dielectric characterization of pure and EDTA doped tris-glycine zinc chloride single crystals for LiDAR. Opt – Int J Light Electron Opt 2016;127(3):1378–83.

[21] Das SJ, Mary Linet J. Optical studies on glycine sodium nitrate: a semiorganic nonlinear optical crystal. Optik (Stuttg) 2012;123(20):1895–9.

[22] Sivakumar N, Jayaramakrishnan V, Baskar K, Anbalagan G. Synthesis, growth and characterization of γ-glycine – a promising material for optical applications. Opt Mater (Amst) 2014;37(C):780–7.

[23] Bharathi MD, Ahila G, Mohana J, Chakkaravarthi G, Anbalagan G. Structural, optical, thermal and mechanical characterization of an organic nonlinear optical material: 4-methyl-3-nitrobenzoic acid single crystal. J Phys Chem Solids 2016;98(4):290–7.

[24] Silambarasan A, Krishna Kumar M, Thirunavukkarasu A, Mohan Kumar R, Umarani PR. Synthesis, crystal growth, solubility, structural, optical, dielectric and microhardness studies of Benzotriazole-4-hydroxybenzoic acid single crystals. J Cryst Growth 2015;420:11–6.

[25] Rajesh K, Kumar PP. Linear and nonlinear optical studies on novel NLO BaTr single crystal. Int J Sci Res 2014;3(8):799–802.

[26] Charoen-in U, Manyum P. Growth of ferroelectric crystals: 4-Aminopyridinium hydrogen maleate single crystals and their characterization. Ceram Int 2015;41:S76–80.

[27] Peter ME, Ramasamy P. Growth of gamma glycine crystal and its characterisation. Spectrochim Acta – Part A Mol Biomol Spectrosc 2010;75(5):1417–21.

[28] Perlovich AB-BGL, Hansen LK. The polymorphism of glycine thermochemical and structural aspects. J Therm Anal Calorim 2001;66:699–715.

[29] Sagadevan S. Growth, Optical and electrical studies of non-linear optical crystal. Optik (Stuttg) 2014;125:950–3.

[30] Debasis D, Tanmay GK, Panchanan P. Studies of dielectric characteristics of BaBi2Nb2O9 ferroelectrics prepared by chemical precursor decomposition method. Solid State Sci 2007;9(1):57–64.

[31] Packkiya Raj M, Ravi Kumar SM, Sreeevasan R, Ravisankar R. Synthesis, growth, and structural, optical, mechanical, electrical properties of a new inorganic non-linear optical crystal: sodium manganese tetrachloride (SMTC). J Taibah Univ Sci 2015;11(1):76–84.

[32] Karolin CKMA, Jayakumari K. Dielectric properties of pure and Ni2+ doped glycine sodium sulfate crystals. Int J Res Eng Technol 2013;2(12):2321–7308.

[33] Saxena P, Dar MA, Sharma P, Kumar A, Varshney D. Structural, dielectric and ferroelectric properties of La and Ni codoped BiFeO3. AIP Conf Proc 2016;1728(1). https://doi.org/10.1063/1.4946358. 020307.

[34] Vizhi RE, Yogambal C. Investigations on the growth and characterization of γ-glycine single crystal in the presence of sodium bromide. J Cryst Growth 2016;452:198–203.

[35] Aliane A, Benwadih M, Bouthinon B, Coppard R, Domingues-Dos Santos F, Daami A. Impact of crystallization on ferro-, piezo- and pyro-electric characteristics in thin film P(VDF-TrFE). Org Electron Physics Mater Appl 2015;25:92–8.

[36] Surekha R, Sagayaraj P, Ambujam K. Third order nonlinear optical, luminescence and electrical properties of bis glycine hydrobromide single crystals. Opt Mater (Amst) 2014;36(5):945–9.

[37] Arun KJ, Jayalekshmi S. Growth and characterisation of nonlinear optical single crystals of L-alaninium oxalate. J Miner Mater Charact Eng 2009;8(8):635–46.